Solid State Communications 149 (2009) 1587–1590

Contents lists available at ScienceDirect

Solid State Communications

journal homepage: www.elsevier.com/locate/ssc

Study on the $K_3Li_2Nb_5O_{15}$ formation during the production of $(Na_{0.5}K_{0.5})_{(1-x)}Li_xNbO_3$ lead-free piezoceramics at the morphotropic phase boundary

Amauri J. Paula [a,*], Rodrigo Parra [b], Maria A. Zaghete [a], José A. Varela [a]

[a] Liec - Instituto de Química, São Paulo State University (UNESP), Rua Prof. Francisco Degni, s/n, 14.801-970, P.O. Box 355, Araraquara, SP, Brazil

[b] Instituto de Investigaciones en Ciencia y Tecnología de Materiales (INTEMA, CONICET-UNMdP), J.B. Justo 4302, B7608FDQ - Mar del Plata, Argentina

ARTICLE INFO

Article history:
Received 28 October 2008
Accepted 30 June 2009 by B.-F. Zhu
Available online 3 July 2009

PACS:
77.84.Dy

Keywords:
A. Ferroelectrics
D. Piezoelectricity
D. Electrostriction
D. Dielectric response

ABSTRACT

Because of the environmental concerns, the manufacture of ceramics based on lead titanate zirconate $[Pb(Zr_{1-x}Ti_x)O_3$ — PZT] has been condemned because of the lead toxicity. In this context, the electromechanical properties of sodium, potassium and lithium niobate $[(Na_{0.5-x/2}K_{0.5-x/2}Li_x)NbO_3$ — NKLN] at the morphotropic phase boundary granted these materials the position of most suitable candidate to replace PZT. However, the production of these ceramics is rather critical mainly because of a natural tendency of forming secondary phases. To help with the studies of the synthesis of this lead-free piezoceramic, this work presents an evaluation of the crystallization of the $(Na_{0.47}K_{0.47}Li_{0.06})NbO_3$ phase by solid-state reactions. TG-DTA, XRD, dilatometric and ferroelectric hysteresis analyses indicated that a secondary phase ($K_3Li_2Nb_5O_{15}$) crystallizes at temperatures above 850 °C and also during the sintering of the powders compacts at 1080 °C. To prevent the formation of this phase, the addition of $Na_2Nb_2O_6.nH_2O$ microfibers obtained through a microwave hydrothermal synthesis was performed in the sintering process. After to this addition, the suppression of the $K_3Li_2Nb_5O_{15}$ phase occurred and an increase of the NKLN electrical properties was then obtained.

1. Introduction

Although lead titanate zirconate piezoceramics $[Pb(Zr_{1-x}Ti_x)O_3$ —PZT] are still the most manufactured in the world mainly because of their great piezoelectric properties [1,2], recent environmental concerns regarding the lead toxicity make the use of this element less attractive. However, the substitution of lead-based materials is quite complex due to difficulties in producing ceramics with similar piezoelectric responses. Basically, researchers have been focusing their studies on alkali niobates, modified bismuth titanates and others solid solutions with compositions at the morphotropic phase boundaries (MPB) [3–9].

Among the studied lead-free piezoceramics, only sodium, potassium and lithium niobate based materials $[(Na_{0.5-x/2}K_{0.5-x/2}Li_x)NbO_3$ —NKLN] were considered proper candidates to substitute PZT [10–14]. In compositions next to the morphotropic phase boundary, NKLN systems present a d_{33} coefficient (induced charge per unit force applied) higher than 230 pC/N and a k_p (planar coupling coefficient) value of 0.42 [10], which were the best piezoelectric properties reported for a normal sintered lead-free piezoceramic [15]. Furthermore, the greatest advance was achieved via the texturization of these ceramics through a Reactive Templated Grain Growth process (RTGG), wherein a promising material with properties similar to PZT4 was obtained (d_{33} = 416 pC/N and k_p = 0.61) [15].

Despite the important discoveries about NKLN materials, as far as the authors know, the literature is lacking of studies reporting on the stability of the $(Na_{0.5-x/2}K_{0.5-x/2}Li_x)NbO_3$ perovskite phase. Considering the sodium instability at high temperatures, the formation of this phase is very delicate inasmuch as there is a natural tendency of forming the $K_3Li_2Nb_5O_{15}$ phase. In this work we propose a study focused on the optimization of the NKLN lead-free ceramic production at the morphotropic phase boundary. In order to avoid the formation of secondary phases, the adequate temperature and time for the formation of $(Na_{0.47}K_{0.47}Li_{0.06})NbO_3$ were analyzed, and also the optimum sintering conditions were determined. Furthermore, an attempt of suppression of the $K_3Li_2Nb_5O_{15}$ phase was tried mixing $Na_2Nb_2O_6{\cdot}nH_2O$ microfibers, obtained through a microwave hydrothermal synthesis, with the NKLN powders produced by solid state reaction.

2. Experimental procedure

$Na_{0.47}K_{0.47}Li_{0.06}NbO_3$ ceramics were prepared by the conventional mixed oxide method. The starting materials were Na_2CO_3 (Mallinckrodt, 99.9%), K_2CO_3 (Mallinckrodt, 99.9%), Li_2CO_3 (Vetec,

* Corresponding author. Tel.: +55 16 33016600x6865.
E-mail address: amauri_jp@yahoo.com.br (A.J. Paula).

0038-1098/$ – see front matter © 2009 Elsevier Ltd. All rights reserved.
doi:10.1016/j.ssc.2009.06.041

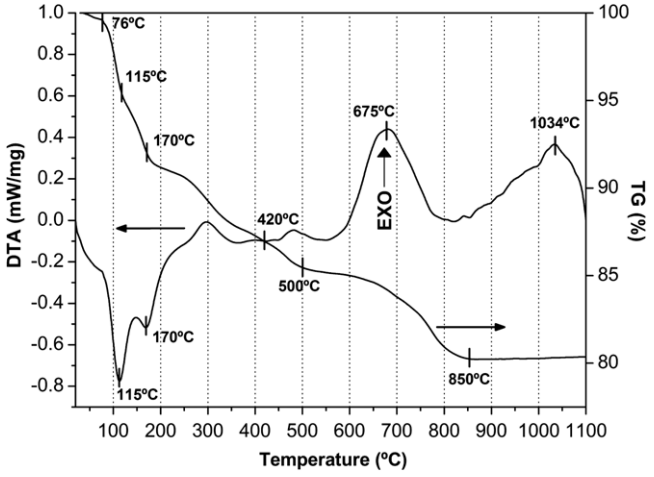

Fig. 1. TG and DTA curves of the raw-materials in air.

99.9%) and Nb_2O_5 (Alfa Aesar, 99.95%). Initially, the raw-materials were mixed for 24 h inside a polyethylene vessel with ZrO_2 balls and ethanol as the medium. After drying, the mixture was calcinated at 850, 900 and 950 °C for 10 h to evaluate the perovskite phase formation. In order to prevent the secondary phase formation during the sintering, NKLN powders calcined at 850 °C for 10 h were ball-milled again in the same conditions described above, dried and then mixed to $Na_2Nb_2O_6{\cdot}nH_2O$ microfibers in 1.0, 3.0 and 5.0 wt.%. The microfibers production is described elsewhere [16]. Later, isobutyl methacrylate (IBMA) was added as a binder and these mixed powders were pressed into disks of 12 mm (diameter) by uniaxial pressing at 30 MPa, followed by cold isostatic-pressing (CIP) at 200 MPa. The binder was burnt at 650 °C for 1 h, and then the sintering process was carried out on the best conditions pointed by dilatometric studies (1080 °C for 4 h). The final bulk densities of the pellets were measured by the Archimedes method.

The crystalline structure was characterized by means of X-ray diffraction (XRD) using a Rigaku equipment (Rotaflex, 50 kV, 100 m A, Cu Kα). The evolution of the solid state reaction between Na_2CO_3, K_2CO_3, Li_2CO_3 and Nb_2O_5 was analyzed by Differential Thermal Analysis (DTA) and Thermo-Gravimetric analysis with a Netzsch/Thermische Analyse equipment with a TASC 414/2 controller, by using a heat rate of 10 °C/min and a synthetic air flux of 30 cm^3/min. A horizontal dilatometer furnace (Netzsch/ Thermische Analyse equipment with TASC 414/2 controller) with a heating rate of 5 °C/min was used to assess the sintering behavior of the pellets and the consequences of this process in the final ceramic density. The NKLN powder and ceramic morphologies were visualized by means of scanning electron microscopy (SEM) using a Topcon/ SM-300 microscope. Measurements of capacitance and dissipation factor as a function of the temperature were registered at 10 kHz using an HP 3457A impedance analyzer coupled to a oven furnace (Maitec, Brazil). To obtain the ferroelectric hysteresis loops, the ceramics were poled under a high voltage (2.5–3.5 kV) at a frequency of 250 Hz during 4ms with a Radiant RT66A polarizer.

3. Results and discussion

The reaction between the alkaline carbonates and niobium pentoxide towards the formation of $(Na_{0.47}K_{0.47}Li_{0.06})NbO_3$ was followed by Differential Thermal Analysis (DTA) and Thermo-Gravimetric analysis (TG), and the results are represented in Fig. 1. As sodium and potassium carbonates are rather hygroscopic salts, the physically and chemically adsorbed waters are liberated at 115 and 170 °C, respectively. However, as observed in the TG curve (Fig. 1), the complete dehydration and decomposition of residual organics, both incorporated in the powders during the milling step, occur at temperatures next to 400 °C. Discarding this weight-loss related to the elimination of water and organics, another loss is related only to the elimination of CO_2 during the decomposition of the carbonates, which represents a weight-loss of 6.75%. Considering the complete decomposition of the carbonates at 850 °C, where the TG curve achieves the minimum value (80.2%), the beginning of the CO_2 elimination would occur exactly at 420 °C (∼86.9%). Among the carbonates, Na_2CO_3 is the less stable and starts to lose CO_2 at lower temperatures (400 °C) than the others [17]. In this way, the weight loss observed just after 400 °C could be associated with the decomposition of Na_2CO_3. Indeed, the CO_2 loss originated from the Na_2CO_3 decomposition was previously identified by mass spectrometry measurements which indicated the decomposition of this compound even at temperatures lower than 400 °C [18].

Although the melting point of lithium carbonate is known to be around 723 °C [17], the thermal decomposition of a small quantity of Li_2CO_3 (13%-mol) into Li_2O drops this temperature to 702 °C due to the presence of an euthetic point in the Li_2CO_3– Li_2O phase diagram [19]. In this context, the endothermic events associated with the lithium carbonate melting and decomposition of Na_2CO_3, K_2CO_3 and Li_2CO_3 occur concomitantly with the exothermic crystallization of the $(Na_{0.47}K_{0.47}Li_{0.06})NbO_3$ perovskite phase. However, as the crystallization reaction is energetically favored, only the exothermic event related to the NKLN formation is seen in the DTA curve at 675 °C. After this event (above 800 °C), another exothermic peak with maximum at 1034 °C appears in the DTA curve, which is related to the crystallization of a secondary phase originated from the decomposition of $(Na_{0.47}K_{0.47}Li_{0.06})NbO_3$, that will be further discussed.

The NKLN perovskite phase formation was confirmed through XRD analyses of the powders calcined at 850, 900 and 950 °C for 10 h (Fig. 2a). The crystallographic indexing for the 850 and 950 °C products was done according to the ABO_3 perovskite subcell of orthorhombic and tetragonal structures, respectively [20], once a transition between these two phases according to the calcination temperature was observed. The $K_3Li_2Nb_5O_{15}$ secondary phase of tungsten bronze structure (ICDD 52-0157) is indexed in Fig. 2a. Whereas the quantification of this secondary phase through a relationship between the most intense peaks of the $(Na_{0.47}K_{0.47}Li_{0.06})NbO_3$ and $K_3Li_2Nb_5O_{15}$ patterns cannot be done because of their overlapping at ∼22.4°, its presence was confirmed by analyzing its characteristic peaks from 23 to 31° (indicated by arrows) [10,12]. Although no peaks related to the $K_3Li_2Nb_5O_{15}$ phase were found in powders produced at 850 °C, the absence of this phase cannot be completely neglected basing on the XRD results. A study on the calcination times at 850 °C indicated that periods either shorter or longer than 10 h increased the $K_3Li_2Nb_5O_{15}$ amount in the powders (Fig. 2b). The presence of $KNbO_3$ at 22.0° (1), $LiNbO_3$ at 23.7° (2), Nb_2O_5 at 29.6° (3) and $NaNbO_3$ at 32.4° (4) was observed just in the powders calcined for 2.5 and 5.0 h (Fig. 2b). Consequently, $NaNbO_3$, $KNbO_3$ and $LiNbO_3$ crystallize simultaneously with (Na, K, Li)NbO_3 and, at a proper temperature, react themselves to form the solid solution. Indeed, the presence of these end-members was previously reported only for powders calcined at lower temperatures than those established as ideal for the formation of the NKLN solid solution [21].

The $(Na_{0.47}K_{0.47}Li_{0.06})NbO_3$ powders produced at 850 °C for 10 h were pressed and underwent a dilatometric study in order to evaluate the proper sintering conditions. The results are shown based on the Linear Retraction Rate, which is the derivation of dL/L_0, where dL is the linear retraction (mm) and L_0 is the initial length of the pellet (mm). As seen in Fig. 3a, a differentiation

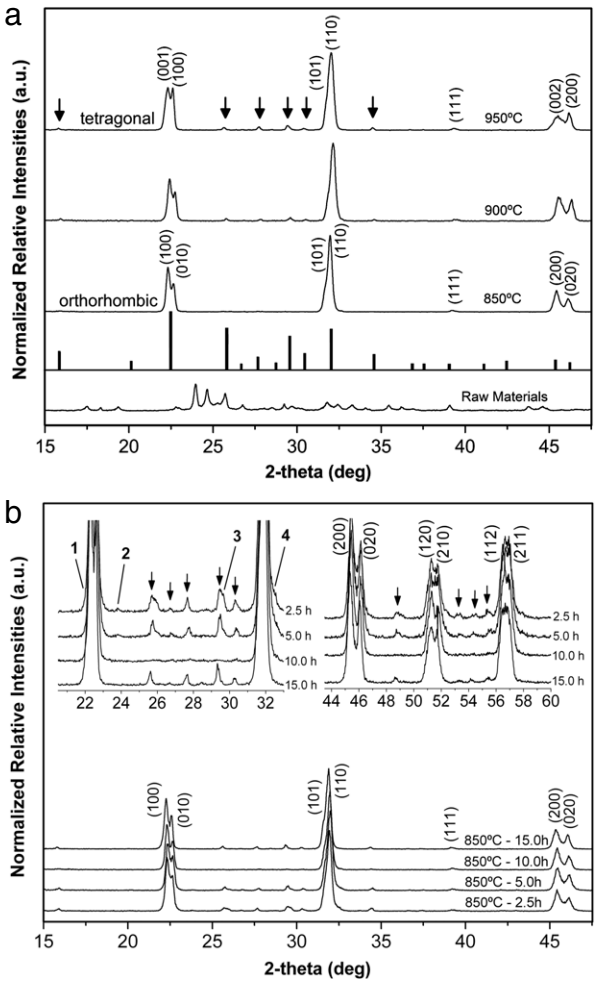

Fig. 2. XRD patterns of the NKLN powders calcined (a) at different temperatures for 10 h and (b) at 850 °C for different times. Phases are indicated as follows: $K_3Li_2Nb_5O_{15}$ (arrows), $KNbO_3$ (1), $LiNbO_3$ (2), Nb_2O_5 (3) and $NaNbO_3$ (4).

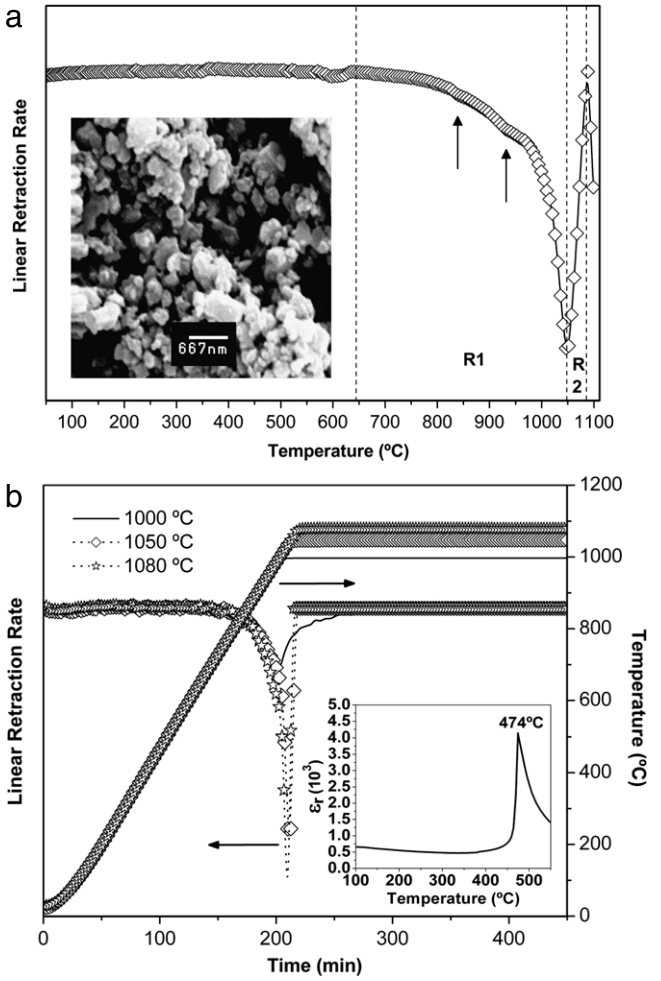

Fig. 3. Dilatometric studies of the NKLN compacts calcined at 850 °C for 10 h: (a) linear retraction rate as a function of the temperature (a SEM image of the NKLN powder is inserted and the liquid phases are indicated by arrows). (b) linear retraction rate and temperature as a function of the time for NKLN ceramics sintered at three different isotherms during 4 h (permittivity values of the NKLN ceramic sintered at 1080 °C for 4 h are inserted).

between the sintering of particles and agglomerates in the first stage of the process (R1 region) was not observed because of the narrow particle size distribution achieved after the milling process (Fig. 3a inset). Furthermore, the sodium and potassium liquid phase formation (represented by arrows) contribute significantly to the sintering process. After ending the grain growth step (R2 region) at 1087 °C, there is a sudden decrease of the $d(dL/L_0)$ values, which is associated with the ceramic degradation. This result explains the higher d_{33} values observed in NKLN ceramics sintered at 1090 °C [22]. As there is a very narrow temperature range that separates the grain growth process and degradation, a precise temperature control must be done to provide high densifications without damaging the electrical properties. Besides, by analyzing the dilatometric behavior of the ceramic pieces after 4 h of sintering at 1000, 1050 and 1080 °C (Fig. 3b), it is possible to verify the compacts stability even during 4 h of isotherm. However, only discs sintered at 1080 °C reached densities greater than 4.30 g/cm^3 (∼96%). According to the ferroelectric–paraelectric transition temperature (474 °C) observed in the Fig. 3b inset, which is exactly the same pointed for $(Na_{0.5-x/2}K_{0.5-x/2}Li_x)NbO_3$ systems at the morphotropic phase boundary ($x = 0.06$) [10], it is possible to conclude that after 4 h of sintering at 1080 °C the stoichiometry of the $(Na_{0.47}K_{0.47}Li_{0.06})NbO_3$ solid solution is maintained.

$K_3Li_2Nb_5O_{15}$ peaks in the region from 21 to 31° which were not observed in the powders produced at 850 °C for 10 h (Fig. 2a and b) appeared in the XRD analyses of the sintered ceramics. By attempting to eliminate this secondary phase from the ceramics, $Na_2Nb_2O_6{\cdot}nH_2O$ single crystalline microfibers produced by hydrothermal synthesis were mixed to $(Na_{0.47}K_{0.47}Li_{0.06})NbO_3$ powders. This material was chosen mainly because of the metastable character of this phase, once it is an intermediary product during the $NaNbO_3$ crystallization. In this way, it would react easier with $K_3Li_2Nb_5O_{15}$. Besides, the sub-micrometric size of these particles (∼200 nm) and their low tendency of agglomerating when produced under specific conditions [16] would also favor the diffusion of this material during the sintering process. As expected, a dilatometric study indicated that the microfibers influence on the shrinkage of the NKLN compacts is very low, considering that all the $Na_2Nb_2O_6{\cdot}nH_2O$-added samples presented the same behavior of the pure NKLN ceramic sintered at 1080 °C for 4 h (Fig. 3b). Indeed, the $Na_2Nb_2O_6{\cdot}nH_2O$ microfibers acted on the elimination of the characteristic peaks of the $K_3Li_2Nb_5O_{15}$ phase (Fig. 4), and consequently, caused an enhancement of the remaining polarization values (P_r), being these: 8.2 μC/cm^2 for the pure NKLN ceramic, and 9.9, 14.9 and 18.9 μC/cm^2 for ceramics with 1.0, 3.0 and 5.0 wt% of $Na_2Nb_2O_6{\cdot}nH_2O$, respectively (Fig. 4 inset). However, a $NaNbO_3$ excess formed through the decomposition of the microfibers did not diffuse into the matrix. This fact is confirmed by the ferroelectric hysteresis curves (Fig. 4 inset), wherein ceramics with

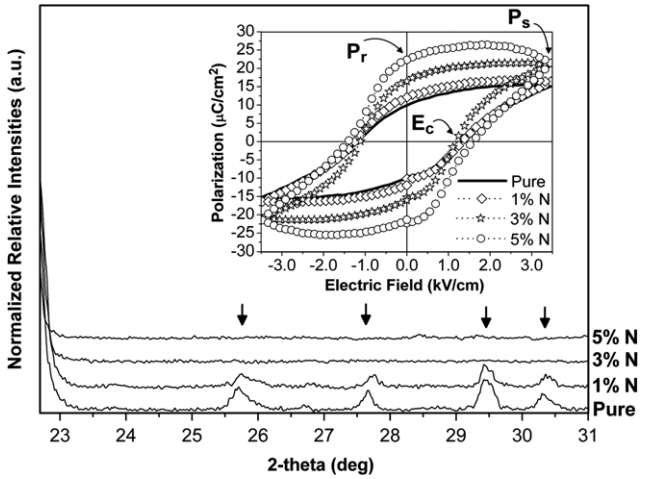

Fig. 4. XRD patterns of pure and $Na_2Nb_2O_6{\cdot}nH_2O$-added NKLN ceramics sintered at 1080 °C for 4 h ($K_3Li_2Nb_5O_{15}$ is indicated by arrows and ferroelectric hystereses of these samples are inserted).

5 wt% of $Na_2Nb_2O_6{\cdot}nH_2O$ (5% N) presented remnant polarization values (P_r) greater than the saturation polarization values (P_s). As $NaNbO_3$ is an anti-ferroelectric material, its individual dipoles arrange antiparallelly to adjacent dipoles when under influence of an electric field, so that the net spontaneous polarization is zero. By quenching the electric field applied over the ceramic, the $NaNbO_3$ ferroelectric domains change their arrangement, and consequently, part of the dipoles align parallelly to the $(Na_{0.47}K_{0.47}Li_{0.06})NbO_3$ oriented ferroelectric domains, resulting in an increase of the polarization values (Fig. 4 inset).

The morphology of all NKLN ceramics was seen by analyzing the fractures of the compact bodies through scanning electronic microscopy (SEM). The addition of the $Na_2Nb_2O_6{\cdot}nH_2O$ microfibers did not cause visible changes in the ceramic grains morphology (Fig. 5a and b). As a natural characteristic, sodium and potassium niobates have a broad grain size distribution and cubic shaped grains. However, as seen in Fig. 5a, the bigger grains (>5 μm) have a greater tendency of suffering intra-granular fracturing. This fact is related to the liquid phase formation during the sintering process, which induces the intra-granular fractures by binding the grains after the solidification. As a consequence, a decrease of the grain surface energy happens and the ceramic fracture occurs at the grain defects and not on its surface.

4. Conclusions

A $(Na_{0.5-x/2}K_{0.5-x/2}Li_x)NbO_3$ (NKLN) solid solution at the morphotropic phase boundary ($x = 0.06$) was produced through the reaction between alkaline carbonates (Na_2CO_3, K_2CO_3 and Li_2CO_3) and niobium pentoxide (Nb_2O_5) at 850 °C, temperature wherein a total decomposition of alkaline carbonates was identified by TG-DTA. By using higher temperatures (900 and 950 °C), the $K_3Li_2Nb_5O_{15}$ secondary phase forms through the decomposition of $(Na_{0.47}K_{0.47}Li_{0.06})NbO_3$. Furthermore, calcination times either greater or lower than 10 h at 850 °C (2.5, 5.0 and 15.0 h) also yielded powders with this secondary phase; however, only for those calcined during 2.5 and 5.0 h, the presence of unreacted $KNbO_3$, $LiNbO_3$, $NaNbO_3$ and Nb_2O_5 was observed with $K_3Li_2Nb_5O_{15}$. Although no peaks related to $K_3Li_2Nb_5O_{15}$ were found in the $(Na_{0.47}K_{0.47}Li_{0.06})NbO_3$ powders produced at 850 °C for 10 h, the ceramics sintered at 1080 °C for 4 h presented a small quantity of this secondary phase. In order to avoid the formation of this undesired phase and consequently enhance the electrical properties of the ceramic, a mixture between $Na_2Nb_2O_6{\cdot}nH_2O$ microfibers and $(Na_{0.47}K_{0.47}Li_{0.06})NbO_3$ powders was successfully used during the sintering process.

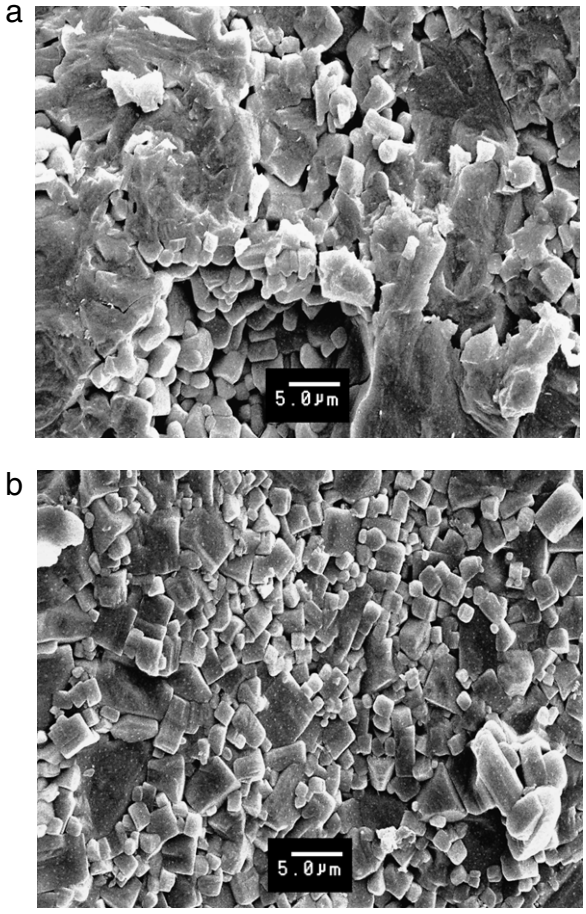

Fig. 5. SEM images of NKLN ceramics sintered at 1080 °C for 4 h: (a) pure and (b) 5% N.

Acknowledgement

This research was funded by a grant from the Fapesp Brazilian Agency.

References

[1] B. Jaffe, R.S. Roth, S. Marzullo, J. Res. Natl. Bur. Stand. 55 (1955) 239.
[2] B. Jaffe, W.R. Cook, H. Jaffe, Piezoelectric Ceramics, Academic Press, New York, 1971.
[3] E. Ringgaard, T. Wurlitzer, J. Eur. Ceram. Soc. 25 (2005) 2701.
[4] Y. Guo, K.-I. Kakimoto, H. Ohsato, Solid. State Commun. 129 (2004) 279.
[5] Z. Yang, B. Liu, L. Wei, Y. Hou, Mater. Res. Bull. 43 (2008) 81.
[6] Q. Xu, S. Wu, S. Chen, W. Chen, J. Lee, J. Zhou, H. Sun, Y. Li, Mater. Res. Bull. 40 (2005) 373.
[7] X.X. Wang, H.L.W. Chan, C.L. Choy, J. Am. Cer. Soc. 86 (2003) 1809.
[8] F. Arai, K. Motoo, T. Fukuda, K. Kato, Appl. Phys. Lett. 85 (2004) 4217.
[9] Y.-M. Li, W. Chen, J. Zhou, Q. Xu, H. Sun, R. Xu, Mat. Sci. Eng. B-Solid 112 (2004) 5.
[10] Y.P. Guo, K. Kakimoto, H. Ohsato, Appl. Phys. Lett. 85 (2004) 4121.
[11] E. Hollenstein, M. Davis, D. Damjanovic, N. Setter, Appl. Phys. Lett. 87 (2005) 182905.
[12] Y. Guo, K.-I. Kakimoto, H. Ohsato, Mater. Lett. 59 (2005) 241.
[13] M. Matsubara, K. Kikuta, S. Hirano, J. Appl. Phys. 97 (2005) 114105.
[14] G.-Z. Zang, J.-F. Wang, H.-C. Chen, W.-B. Su, C.-M. Wang, P. Qi, B.-Q. Ming, J. Du, L.-M. Zheng, S. Zhang, T.R. Shrout, Appl. Phys. Lett. 88 (2006) 212908.
[15] Y. Saito, H. Takao, T. Tani, T. Nonoyama, K. Takatori, T. Homma, T. Nagaya, M. Nakamura, Nature 432 (2004) 84.
[16] A.J. Paula, M.A. Zaghete, E. Longo, J.A. Varela, Eur. J. Inorganic Chem. (2008) 1300.
[17] P. Patnaik, Handbook of Inorganic Chemicals, McGraw-Hill, New York, 2002.
[18] T. Hungria, M. Algueró, A. Castro, Chem. Mater. 18 (2006) 5370.
[19] P. Pasierb, R. Gajerski, S. Komornicki, M. Rekas, J. Therm. Anal. Calorim. 65 (2001) 457.
[20] K. Wang, J.-F. Li, Appl. Phys. Lett. 91 (2007) 262902.
[21] T.A. Skidmore, S.J. Milne, J. Mater. Res. 22 (2007) 2265.
[22] P. Zhao, B.-P. Zhang, J.-F. Li, Scripta Mater. 58 (2008) 429.